

Einstein-Podolsky-Rosen state for space-time variables in a two-photon interference experiment

Y. H. Shih, A. V. Sergienko, and M. H. Rubin

Department of Physics, University of Maryland at Baltimore County, Baltimore, Maryland 21228

(Received 8 January 1992; revised manuscript received 4 September 1992)

A pair of correlated photons generated from parametric down-conversion was sent to two independent Michelson interferometers. Second-order interference was studied by means of a coincidence measurement between the outputs of two interferometers. The reported experiment and analysis studied this second-order interference phenomenon from the point of view of the Einstein-Podolsky-Rosen (EPR) paradox. The experiment was done in two steps. The first step of the experiment used 50-psec and 3-nsec coincidence time windows simultaneously. The 50-psec window was able to distinguish a 1.5-cm optical path difference in the interferometers. The interference visibility was measured to be 38% and 21% for the 50-psec time window and 22% and 7% for the 3-nsec time window, when the optical path differences of the interferometers were 2 cm and 4 cm, respectively. By comparing the visibilities between these two windows, the experiment showed the nonclassical effect which resulted from an EPR state. The second step of the experiment used a 20-psec coincidence time window, which was able to distinguish a 6-mm optical path difference in the interferometers. The interference visibilities were measured to be 59% for an optical path difference of 7 mm. This is an observation of visibility greater than 50% for a two-interferometer EPR experiment which demonstrates nonclassical correlation of space-time variables.

PACS number(s): 42.50.Wm, 03.65.Bz

I. INTRODUCTION

Two-photon interferometry has drawn a great deal of attention recently because it provides a tool to study the foundation of quantum mechanics and the fundamental properties of the electromagnetic field. A two-photon interference experiment using two independent interferometers was proposed by Franson [1], which constituted an Einstein-Podolsky-Rosen (EPR) experiment for space-time variables. Since then several experiments have reported the second-order (second order in intensity, fourth order in field) interference effect [2–5]. These experiments have shown visibility less than 50% when the optical path difference of the interferometers is greater than the coherence length of the optical beam. The reason that the visibilities are less than 50% is due to the use of large coincidence time windows in these experiments. It has been pointed out that classical models predict a maximum of 50% visibility for these experiments [2,3,6]. Quantum theory predicts visibility greater than 50% for certain entangled states we called the EPR states. To make the type of argument presented by EPR [7] this state must be produced. For this experiment a short coincidence time window is needed to prepare an EPR state.

Recently, a large set of measurements for a two-photon interference experiment have been carried out in our laboratory. In this experiment parametric down-conversion is used to produce the correlated two photons. The intensity of the down-converted radiation used for the experiment is sufficiently low so that a two-photon state is produced such that each beam contains at most one photon. Each photon is passed through an independent Michelson interferometer and is then detected by a coincidence counter. If the interferometers are set so that the

optical path differences are longer than the coherence length of the fields, there is no first-order interference (first order in intensity, second order in field). However, there is second-order interference if the optical paths of the two interferometers are approximately equal. The interference arises from the frequency and wave-number correlation in a given pair generated by the phase-matching conditions, $\omega_1 + \omega_2 = \omega_p$ and $\mathbf{k}_1 + \mathbf{k}_2 + \mathbf{k}_p$, where ω_p and \mathbf{k}_p are the pump frequency and wave number. The second-order interference is measured by studying the visibility of the interference fringes that are generated by varying the optical path difference of the interferometers. The visibility of the interference can be estimated by classical and quantum models. The classical model never predicts visibility greater than 50%. However, for idealized conditions, the quantum model predicts a 100% visibility when the coincidence time window is shorter than the optical path difference. In this case, the registration time of one photon traversing the long path and the other following the short path of the interferometers is outside the coincidence window and will not be registered by the coincidence counter. As will be explained below, the use of a short coincidence time window is equivalent to preparing a type of entangled state discussed in the original EPR paper [7].

In this paper we report an experiment which shows second-order interference visibility greater than 50% for two independent interferometers. We also show in detail how the EPR state is generated for the coincidence counting experiment.

II. EPR PARADOX AND EPR STATE

The EPR paradox was based on the argument that noncommuting observables can have simultaneous reality

[7]. EPR first gave their criterion: if, without in any way disturbing the system, we can predict with certainty (i.e., with probability equal to unity) the value of a physical quantity, then there exists an element of reality corresponding to this physical quantity. The gedanken experiment discussed by Einstein, Podolsky, and Rosen was modified by Bohm in 1951 [8]. In Bohm's version a singlet state $|\psi\rangle$ of two spin- $\frac{1}{2}$ particles is produced by some source,

$$|\psi\rangle = \frac{1}{\sqrt{2}} [|\hat{n}_1^+\rangle \otimes |\hat{n}_2^-\rangle - |\hat{n}_1^-\rangle \otimes |\hat{n}_2^+\rangle], \quad (1)$$

where $|\hat{n}_j^\pm\rangle$ quantum mechanically describe a state in which particle j has spin "up" or "down" along the direction \hat{n} . For this state, if the spin of particle 1 is measured along the x axis, particle 2 will be found to have its spin oppositely aligned along the x axis with unit probability. Thus, the x component of the spin of particle 2 can be measured without in any way disturbing it, and so is an element of reality according to the EPR criterion. It is similarly found that the other components of the spin of particle 2 can be determined as elements of physical reality and must exist without considering which component is being measured. Of course this point of view is different from that of quantum mechanics. Philosophical arguments aside, the predictability of the spin of particle 2 with 100% certainty after measuring the spin of particle 1 is a mathematical consequence of quantum theory applied to state of the form (1). States of type (1) are a particular type of entangled state [9,10], which will be called the EPR state. It is the EPR state which leads to the nonclassical interference behavior of the two-particle system. It is the EPR state that has no classical analog.

The existence of polarization EPR states has been experimentally demonstrated [11–14]. The additional type of EPR experiment considers the measurement of position and time correlation in contrast to the historical measurement of polarization correlation. The key element is to seek an EPR state for space and time variables. This is closer to the original EPR gedanken experiment for the determination of position and momentum of a photon. In this case (see Fig. 1) the two-photon EPR state sought is of the form

$$\Psi_{\text{EPR}} = \Psi(L_1, L_2) + \Psi(S_1, S_2), \quad (2)$$

where the first amplitude corresponds to the photons both passing along the longer arms of the interferometers and the second amplitude corresponds to them both following the shorter arms. It is clear that this is an EPR state of the type defined above, if photon 1 is determined in the long (short) arm, then, photon 2 follows the long (short) path. The photon path is then an element of physical reality according to the EPR criterion. In practice, state (2) is produced by parametric down-conversion. If we assume perfect phase matching, then because $k_1 + k_2 = \text{const}$, a momentum measurement of one photon determines the momentum of the other. So the momentum of the photon is also an element of physical reality. If this state does exist, in idealized conditions, its

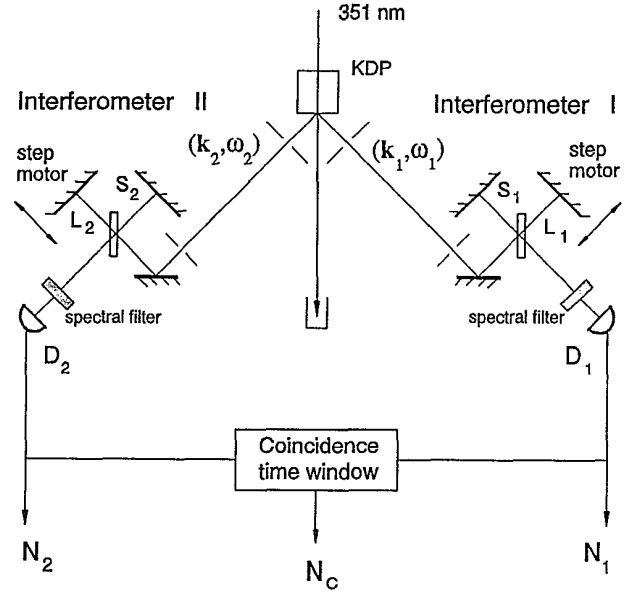


FIG. 1. Schematic diagram of the experiment.

signature is an interference visibility of 100% when the optical path differences of the two independent interferometers are equal.

However, the output of the interferometers is not state (2), but rather the state

$$\Psi = \Psi(L_1, L_2) + \Psi(S_1, S_2) + \Psi(L_1, S_2) + \Psi(S_1, L_2), \quad (3)$$

which differs because of the presence of the last two terms, which correspond to one photon passing the long arm and another passing the shorter arm of the interferometers. State (3) cannot give any determination of the paths of the photon. It gives a maximum of 50% visibility, which cannot be extinguished from a classical model. However, it will be seen in the next section, that according to quantum mechanics, the last two terms of (3) can be suppressed by using a coincidence time window which is shorter than the optical path difference of the interferometers.

III. THEORETICAL DISCUSSION

Our version of the EPR experiment is illustrated in Fig. 1. The photon pair generated from parametric down-conversion is sent through two independent Michelson interferometers I and II. The optical path differences $\Delta L_1 = L_1 - S_1$ and $\Delta L_2 = L_2 - S_2$ can be arranged to be shorter or longer than the coherence length of each beam of the down-conversion field. The coincidence measurement is between the two outputs of the interferometers.

The two-photon state of the parametric down-conversion can be considered as

$$\Psi = \int dk_1 \int dk_2 \delta(k_1 + k_2 - k_p) A(k_1) |k_1\rangle \otimes |k_2\rangle, \quad (4)$$

where k_1 is the signal, k_2 is the idler, and k_p is the pump wave number; the δ function comes from the perfect phase-matching condition of the parametric down-conversion, $A(k)$ is the wave-packet distribution func-

tion, and its width determines the coherence length of the wave packet. After leaving the interferometers, the wave function becomes

$$\begin{aligned} \Psi = & \frac{1}{4} \int dk_1 \int dk_2 \delta(k_1 + k_2 - k_p) A(k_1) \\ & \times [|k_{1L}\rangle |k_{2L}\rangle + |k_{1S}\rangle |k_{2S}\rangle \\ & + |k_{1L}\rangle |k_{2S}\rangle + |k_{1S}\rangle |k_{2L}\rangle], \end{aligned} \quad (5)$$

where $|k_{iM}\rangle = |k_i\rangle_S e^{i\phi(Mi)}$, ϕ is the phase shift caused by passage of the wave through the system. The four terms of state (5) correspond to the photons which have followed the long-long, short-short, long-short, and short-long paths of the interferometers. State (5) is not an EPR state; the coincidence rate can be estimated as $R_c = R_{c0} |\Psi|^2$,

$$\begin{aligned} R_c = R_{c0} \int dk_1 F(k_1) \{ & 1 + \cos k_1 \Delta L_1 + \cos(k_p - k_1) \Delta L_2 \\ & + \frac{1}{2} \cos[k_1(\Delta L_1 + \Delta L_2) - k_p \Delta L_2] \\ & + \frac{1}{2} \cos[k_1(\Delta L_1 - \Delta L_2) + k_p \Delta L_2] \}, \end{aligned} \quad (6)$$

where $|A(k_1)|^2 \equiv F(k_1)$. Function $F(k_1)$ will generally have about the same width as $|A(k)|^2$. If ΔL_1 and ΔL_2 are greater than the first-order coherence length of the wave packets, the second, third, and fourth terms in (6) will vanish. The last term contains $\cos[k_1(\Delta L_1 - \Delta L_2) + k_p \Delta L_2]$; consequently, so long as $|\Delta L_1 - \Delta L_2|$ is less than the first-order coherence length of the wave packet, this term gives rise to the interference fringes. If $|\Delta L_1 - \Delta L_2|$ is much less than the coherence length (equal optical path difference) then the visibility of these fringes attain their maximum value of 50%.

A similar result can be obtained from a classical model [6,15]. In the classical analog to the above experiment the electric field leaving the interferometer i will be

$$E_i = \int dk_i A(k_i) e^{i(k_i r - \omega_i t)} (1/\sqrt{2}) (e^{i\phi(L_i)} + e^{i\phi(S_i)}), \quad (7)$$

where we neglect the polarization vector. The intensity is given by

$$I_i = \int dk_i |A_i(k_i)|^2 \frac{1}{2} (1 + \cos \delta_i), \quad (8)$$

where $\delta_i = k_i \Delta L_i = \phi(L_i) - \phi(S_i)$. The modulation as a function of the optical path difference ΔL_i is determined by the width of the function $|A_i(k_i)|^2$ and gives the first-order interference coherence length of the field.

Now suppose the second-order interference is measured, the coincidence counting rate $R_c \propto \langle I_1 I_2 \rangle$, where the angular brackets denote an ensemble average,

$$\begin{aligned} \langle I_1 I_2 \rangle = & \int dk_1 \int dk_2 \langle |A_1(k_1)|^2 |A_2(k_2)|^2 \rangle \\ & \times \cos^2(k_1 \Delta L_1 / 2) \cos^2(k_2 \Delta L_2 / 2). \end{aligned} \quad (9)$$

In order to model parametric down-conversion it is necessary to account for the correlation in the two beams that is imposed by the phase-matching condition. To do this assume perfect phase matching and take

$$\langle |A_1(k_1)|^2 |A_2(k_2)|^2 \rangle = \delta(k_1 + k_2 - k_p) G(k_1),$$

so that

$$\begin{aligned} R_c = R_{c0} \int dk_1 G(k_1) \{ & 1 + \cos k_1 \Delta L_1 + \cos(k_p - k_1) \Delta L_2 \\ & + \frac{1}{2} \cos[k_1(\Delta L_1 + \Delta L_2) - k_p \Delta L_2] \\ & + \frac{1}{2} \cos[k_1(\Delta L_1 - \Delta L_2) + k_p \Delta L_2] \}. \end{aligned} \quad (10)$$

It is the same as (6), which we have derived from the state (5).

It is not surprising that a classical model gives the same answer as that of quantum mechanics, because the above calculations have dealt with the wave nature of radiation for both the quantum and the classical models. However, if one can take advantage of the particle nature of the photon, the quantum prediction will be different. This idea has been demonstrated in the early polarization EPR experiment using a coincidence measurement to produce an EPR state [13]. For the two-photon interference experiment a coincidence measurement is not enough to suppress the last two terms of (5) unless the coincidence time window is shorter than the optical path difference of the interferometers. Then the registration time difference in which the photons follow the long-short and short-long paths are outside the time window, i.e., the last two terms of (5) will not be registered by the coincidence counter [16]. This ‘‘cutoff’’ effect will result in an EPR state, which has no classical analog,

$$\begin{aligned} \Psi = & \frac{1}{4} \int dk_1 \int dk_2 \delta(k_1 + k_2 - k_p) A(k_1) \\ & \times [|k_{1L}\rangle |k_{2L}\rangle + |k_{1S}\rangle |k_{2S}\rangle]. \end{aligned} \quad (11)$$

The EPR state (11) can provide 100% interference visibility,

$$R_c = R_{c0} \int dk_1 F(k_1) \{ 1 + \cos[k_1(\Delta L_1 - \Delta L_2) + k_p \Delta L_2] \}. \quad (12)$$

To realize 100% visibility, besides equal optical path difference in the interferometers, a pump field with zero bandwidth is required along with perfect phase matching for the parametric down-conversion. One can easily arrange a narrow enough spectral bandwidth of the pump field by means of a single mode laser as was done in this experiment, but, in principle, it is impossible to achieve perfect phase matching. When the finite size of the crystal and the finite interaction time of the down-conversion is taken into account, the δ functions of $k_1 + k_2 - k_p$ and $\omega_1 + \omega_2 - \omega_p$ are replaced by functions with nonzero widths, giving $k_1 + k_2 = k_p \pm \Delta k$ and $\omega_1 + \omega_2 \pm \Delta \omega$ [17]. In this case (12) becomes

$$\begin{aligned} R_c = R_{c0} \int dk_1 F(k_1) \{ & 1 + \cos[k_1(\Delta L_1 - \Delta L_2) \\ & + k_p \Delta L_2 \pm \Delta k \Delta L_2] \}. \end{aligned} \quad (13)$$

The uncertainty Δk will reduce the interference visibility.

A detailed and careful study of the influence of the coincidence time window and the nonperfect phase

matching can be found in Ref. [6]. For a quasimono-chromatic wave model, which is reasonable for parametric down-conversion, the general solution of R_c may be written as

$$R_c = R_{c0} \{ f_0 + f_1 \cos [k_1 (\Delta L_1 - \Delta L_2) + k_p \Delta L_2] \} \quad (14)$$

where we assume that the optical path difference is much longer than the coherence length of the down-conversion beams and ignore the trivial terms. The f 's depend on the detail of the experiment, in particular the coincidence time window and the uncertainty Δk . For a large coincidence window, f_1/f_0 attains a maximum value of 50%. When the time window becomes shorter and shorter, especially shorter than the optical path difference of the interferometers, f_1/f_0 reaches 100% for zero Δk .

IV. EXPERIMENT

The experimental arrangement is shown in Fig. 1. A 351.1-nm single-mode cw argon laser beam was used to pump a 50-mm-long potassium dihydrogen phosphate (KDP) nonlinear crystal for optical parametric down-conversion. The coherence length of the 351.1-nm pump beam was measured to be longer than 5 m. The KDP crystal was cut at type-I phase matching angle for generation of ω_1 and ω_2 photons. Both degenerate and non-degenerate (in frequency) photon pairs have been used in the experiment. In the degenerate case, $\lambda_1 = \lambda_2 = 702.2$ nm. The emission angles were about 2° relative to the pump. In the nondegenerate case 632.8 and 788.7-nm signal and idler pair were generated. The signal and idler photons were emitted at angles 1.8° and 2.3° relative to the pump beam, respectively. The signal and idler photons then were selected by pinholes and sent to two independent Michelson interferometers I and II. The interferometers are 5 m apart in order to have spacelike separated detections. Two Geiger mode avalanche photodiodes D_1 and D_2 with 1-nm spectral filters (centered at 702.2 nm for the degenerate case and 788.7 and 632.8 nm for nondegenerate cases, respectively) were used for monitoring the first-order and the second-order interferences by means of direct counting and coincidence counting. The coincident circuit provides 20-psec, 50-psec, and 3-nsec time windows. N_1, N_2, N_c , which correspond to the number of counts from detector 1, detector 2, and from the coincidence time window, were recorded simultaneously. The above measurements have taken advantage of the state-of-the-art millimeter lunar laser ranging high-resolution timing diagnostic technique, which has been developed at the University of Maryland.

The optical path differences $\Delta L_1 = L_1 - S_1$ and $\Delta L_2 = L_2 - S_2$ of the two independent Michelson interferometers I and II can be changed by step motors continually from white light condition to about 7.2 mm, which is longer than both the coherence length of the down-converted fields and the 20-psec time window. It is also possible to move one of the mirrors discontinuously to a maximum $\Delta L = 12$ cm.

The experiment was performed in two steps. First, we used a 50-psec and a 3-nsec time window simultaneously for the coincidence measurement. By comparing the in-

terference visibilities for $\Delta L > 1.5$ cm between the 50-psec and 3-nsec coincidence windows, we expect to see the "cutoff" effect. The 702.2-nm photon pairs were used for the first step measurement.

1. ΔL_i less than the coherence length. We have measured the first-order and the second-order interference visibilities when both ΔL_1 and ΔL_2 were shorter than the coherence length of the field. We have also measured the first- and second-order interference visibilities when the optical path difference of one interferometer was shorter than the coherence length and that of the other was much longer than the coherence length. Figures 2(a) and 2(b) show the second-order and the first-order interference visibilities with $\Delta L_2 = 5$ mm and ΔL_1 scanned starting from the white light condition. The 97% second-order and 82% first-order interference visibilities were observed at the beginning of the scan. All reported values are directly measured without noise reduction and theoretical corrections.

2. ΔL_i greater than the coherence length. Figures 3(a) and 3(b) report two typical second-order interference visibility measurements in which ΔL_2 was set to a value that was longer than the coherence length and ΔL_1 was scanned from white light condition. For each data point, the visibility was calculated from measurements similar to those shown in Fig. 2. It is clear that the interference disappeared at about $\Delta L_1 = 500 \mu\text{m}$, which corresponds to the first-order coherence length of the field (determined by the bandwidth of the spectral filter) and reap-

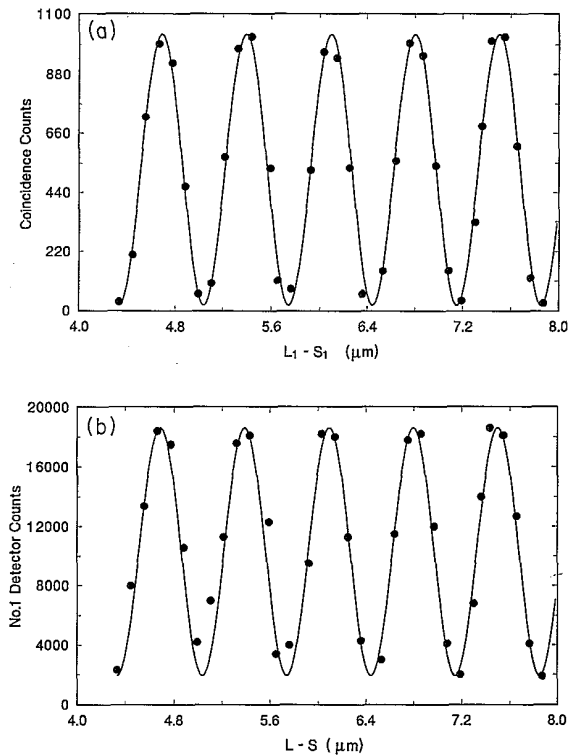


FIG. 2. (a) Second-order interference near white light condition, showing visibility near 100%. (b) First-order interference near white light condition, showing visibility 82% (noise was not subtracted).

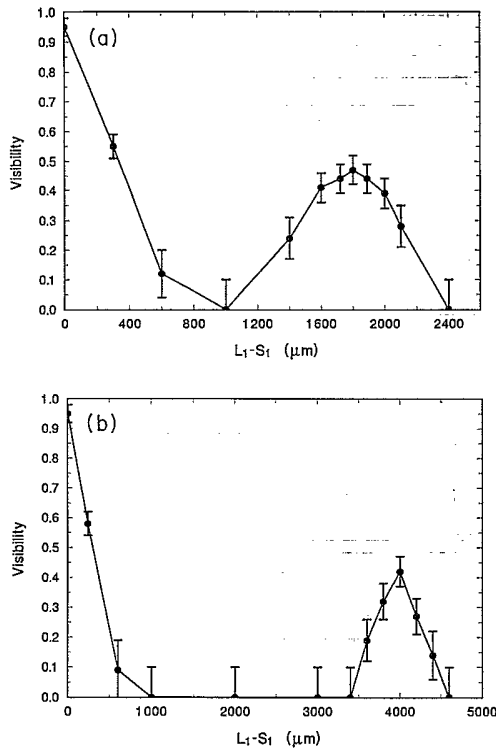


FIG. 3. (a) Second-order interference visibility with 50-psec coincidence window ($\Delta L_2 = 1.8$ mm, ΔL_1 scanned from the white light condition). (b) Second-order interference visibility with 50-psec coincidence window ($\Delta L_2 = 4$ mm, ΔL_1 scanned from white light condition).

peared around $\Delta L_1 = \Delta L_2$. These measurements were repeated many times.

Figure 4 and Table I report the second-order interference visibility measurements for $\Delta L_1 = \Delta L_2$ with the 50-psec time window and the 3-nsec time window. The interference visibilities were measured to be $(38 \pm 6)\%$ and $(21 \pm 7)\%$ for the 50-psec window and $(22 \pm 2)\%$ and $(7 \pm 3)\%$ for the 3-nsec window, when the optical path differences of the interferometers were 2 and 4 cm, respectively. The ratios are about 1.7 ± 0.3 for $\Delta L = 2$ cm and about 3.0 ± 1.6 for $\Delta L = 4$ cm, respectively. The cutoff effect is clearly demonstrated. However, we still

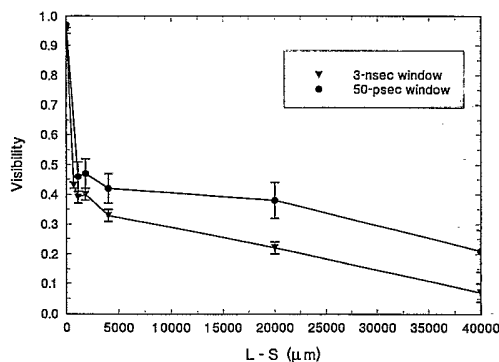


FIG. 4. Second-order interference visibility for equal optical path differences with 50-psec and 3-nsec coincidence time window.

TABLE I. Second-order interference visibility for equal optical path difference ($L_1 - S_1 = L_2 - S_2$) with 50-psec and 3-nsec coincidence time window.

$L-S$ (mm)	3-nsec window	50-psec window	Visibility ratio ($V_{50 \text{ psec}}/V_{3 \text{ nsec}}$)
0	$(95 \pm 1)\%$	$(97 \pm 3)\%$	1.02 ± 0.03
1.1	$(39 \pm 2)\%$	$(46 \pm 5)\%$	1.18 ± 0.14
1.8	$(40 \pm 2)\%$	$(47 \pm 5)\%$	1.17 ± 0.14
4.0	$(33 \pm 2)\%$	$(42 \pm 5)\%$	1.21 ± 0.17
20.0	$(22 \pm 2)\%$	$(38 \pm 6)\%$	1.72 ± 0.32
40.0	$(7 \pm 3)\%$	$(21 \pm 7)\%$	3.00 ± 1.63

need a visibility more than 50% in order to have an unambiguous quantum result.

The second step of the experiment used a 20-psec coincidence time window. Higher interference visibility ($> 50\%$) was expected at $\Delta L > 6$ nm. In this experiment, 632.8- and 788.7-nm photon pairs were used for the measurement. The wavelength 632.8 nm was used for easy alignment. We used a cw He-Ne laser beam as input signal to match the 632.8-nm down-conversion mode. Both 632.8 and 788.7-nm radiation have much longer coherence length due to the stimulated down-conversion (or so-called induced coherence). The parametric amplified signal and idler radiation were used for careful alignment. High-visibility first-order interference of the stimulated down-conversion beams were observed before taking data.

Figures 5–7 report the experimental results. Figure 5 (Fig. 6) is a typical measurement in which ΔL_1 (ΔL_2) was fixed at 7 mm and ΔL_2 (ΔL_1) scanned around 7 mm. Figure 7 reports the measurement in which both interferometers were scanned around 7 mm. The 7-mm optical path difference was much longer than the coherence length of the down-conversion beam; no first-order interference can be observed in N_1 or N_2 ; however, the coincidence measurement N_c showed clear interference fringes in the above measurements. The fringe visibilities are 59% with a period of 632.8 nm and 59% with a period of 788.7 nm for the type of measurements in Figs. 5 and 6, respectively. When both ΔL_1 and ΔL_2 are changed together the visibility is 58% with a period of 351.1 nm. The solid

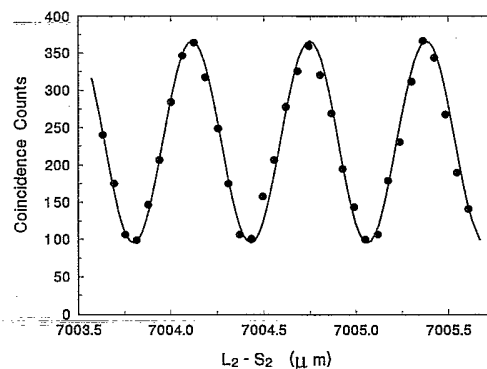


FIG. 5. Second-order interference fringes for 632.8 nm ($\Delta L_1 = 7$ mm, ΔL_2 scanned around 7 mm, 100 sec for each point) with 20-psec coincidence time window.

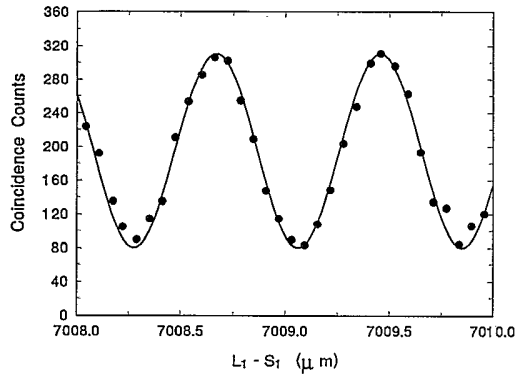


FIG. 6. Second-order interference fringes for 788.7 nm ($\Delta L_2 = 7$ mm, ΔL_1 scanned around 7 mm, 100 sec for each point) with 20-psec coincidence time window.

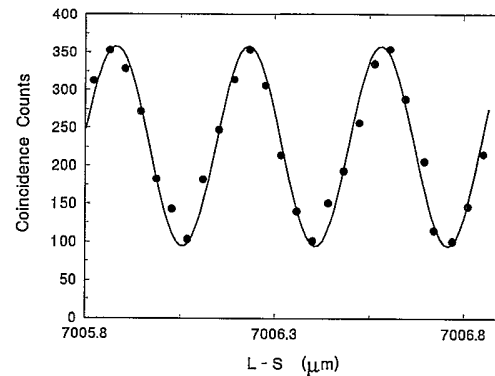


FIG. 7. Second-order interference fringes for 351.1 nm ($\Delta L_1 = \Delta L_2$, ΔL_1 and ΔL_2 scanned together around 7 mm, 100 sec for each point) with 20-psec coincidence time window.

curves in Figs. 5, 6 and 7 are the fittings for 632.6, 788.7, and 351 nm, respectively. The standard deviation for these measurements is about 2%.

V. SUMMARY

(1) The existence of the EPR state has been observed by means of the following.

(i) The cutoff effect, i.e., the interference visibility comparison between the 50-psec and 3-nsec coincidence time windows.

(ii) Direct measurement of more than 50% interference visibility for a 20-psec coincidence time window. This is an observation of visibility greater than 50% for the two independent interferometers experiment.

(2) The second-order interference coherence (second order in intensity, fourth order in field) is not limited by the coherence length of the pump beam only, but also by the nonperfect phase matching of the parametric down-conversion. The uncertainty of the correlation in frequency determines the second-order coherence length. We believe it is the nonperfect phase matching of the down-conversion that reduced the visibility of the second-order interference fringes in our experiment.

ACKNOWLEDGMENTS

We acknowledge many fruitful discussions with C. O. Alley. This work was supported by the Office of Naval Research under Grant No. N00014-91-J-1430.

-
- [1] J. D. Franson, Phys. Rev. Lett. **62**, 2205 (1989).
 [2] P. G Kwiat, W. A. Vareka, C. K. Hong, H. Nathel, and R. Y. Chiao, Phys. Rev. A **41**, 2910 (1990).
 [3] Z. Y. Ou, X. Y. Zou, L. J. Wang, and L. Mandel, Phys. Rev. Lett. **65**, 321 (1990).
 [4] J. D. Franson, Phys. Rev. A **44**, 4552 (1991).
 [5] J. G. Rarity and P. R. Tapster, Phys. Rev. A **45**, 2052 (1992).
 [6] M. H. Rubin and Y. H. Shih, Phys. Rev. A **45**, (1992).
 [7] A. Einstein, B. Podolsky, and N. Rosen, Phys. Rev. **47**, 777 (1935).
 [8] D. Bohn, *Quantum Theory* (Prentice-Hall, Englewood Cliffs, 1951).
 [9] E. Schrödinger, Naturwissenschaften **23**, (1935); **23**, 823 (1935); **23**, 844 (1935). A translation of these papers appears in *Quantum Theory and Measurement*, edited by J. A. Wheeler and W. H. Zurek (Princeton University Press, Princeton, 1983).
 [10] M. A. Horn, A. Shimony, and A. Zeilinger, Phys. Rev. Lett. **62**, 2209 (1989); in *Quantum Coherence*, Proceedings of the International Conference on the Fundamental Aspects of Quantum Theory, edited by G. S. Anandan (World Scientific, Singapore, 1989), p. 356.
 [11] For a review, see J. F. Clauser and A. Shimony, Rep. Prog. Phys. **41**, 1881 (1976).
 [12] A. Aspect, P. Grangier, and G. Roger, Phys. Rev. Lett. **47**, 460 (1981); **49**, 91 (1982); A. Aspect, J. Dalibard, and G. Roger, *ibid.* **49**, 1804 (1982).
 [13] Y. H. Shih and C. O. Alley, Phys. Rev. Lett. **61**, 2921 (1988).
 [14] Z. Y. Ou and L. Mandel, Phys. Rev. Lett. **61**, 50 (1988).
 [15] Z. Y. Ou and L. Mandel, J. Opt. Soc. Am. B **7**, 2127 (1990).
 [16] J. Brendel, E. Mohler, and W. Martienssen, Phys. Rev. Lett. **66**, 1142 (1991). This experiment using a single interferometer and collinear photon beams demonstrated higher visibility with a short coincidence time window.
 [17] For example, A. Yariv, *Quantum Electronics* (Wiley, New York, 1989).